Journal of Multidisciplinary Engineering Science Studies (JMESS)
ISSN: 2458-925X
Vol. 2 Issue 3, March - 2016

Mechanics of a Fluid-Conveying Pipeline System Resting on a Viscoelastic Foundation

Patrick S. Olayiwola
Department of Mechanical & Biomedical Engineering, College of Engineering, Bells University of Technology, Ota, Ogun State 234037, Nigeria

***Abstract*— In this paper, a harmonically-excited fluid-conveying pipeline system resting on a viscoelastic foundation is presented as a boundary value problem of mathematical physics. The static and dynamic states of the system are analytically examined following a direct method process. The static analysis with its interacting and influencing loads reveals the true initial configuration and, after charging the system with dynamic loadings, the functions for the complex and natural frequencies are derived. Then, the dynamic and vibration characteristics of the internal flow trigger fluid-structure interactions on the pipeline segment, which is idealized as an elastic hollow beam. The effect of Coriolis, elastic and damping forces on the overall dynamic response of the system is investigated. On employing integral transforms and complex variable functions, a closed form analytical expression is derived for the overall dynamic response. It is demonstrated that a concise mathematical expression for the natural frequency associated with any mode of vibration can be deduced from the algebraic product of the complex frequency pairs. Analysis for damping decrement physics and associated mathematical expressions are derived to illustrate viscoelastic damping effects on the system's dynamic stability.**

Keywords*— Harmonically-excited pipeline, viscoelastic foundation, direct method , Coriolis and damping forces, integral transforms, complex and natural frequency.*

I. INTRODUCTION (*Heading 1*)

It was pointed out by Paidoussis [1] that the work on the dynamics of pipes conveying fluid is mostly curiosity-driven and that, over the years, it has yielded rich rewards - among which are: (i) the development of theory for certain classes of dynamical systems, and of new analytical methods for such systems; (ii) the understanding of the dynamics of more complex systems (such as the investigation of the dynamics and stability of fluid-conveying curved and twisted pipes in complex spatial forms), and (iii) the direct use of this work in some a priori unforeseen practical applications.

Analyses of these types of problem have employed various solution methods that are usually numerical schemes oriented. However, direct methods such as the integral transforms, are deployable so as to reveal processes of the solution that may provide a systematic exposition of some parameters that were not observable with the use of some of those methods. Examples of such are the frequencies due to Coriolis force and that of the combined Coriolis and damping forces as appeared in this paper. The integral transforms provide powerful operational methods for solving typical initial value problems and initial-boundary value problems for linear differential and integral equations; it also possesses many mathematical and physical applications.

In this paper, it is essential to note that characteristics of coupled oscillators demonstrated are as a result of fluid-conveying pipeline systems exhibiting flow-induced vibrations occur due to the fact that a structure is in contact with flowing fluid, no matter how small the flow velocity may be. The Coriolis force component, which is observed to be acting in phase with the lateral or transverse displacement of the pipe, are among the terms describing the mathematical models of the system displaying coupled oscillations. This term has drawn researchers and engineering physicists into probing its significance within the system. Mostafa (2014) [3] experimentally investigated the natural frequency of a simply supported pipeline (hinged type) conveying 1-D incompressible steady fluid flow set on a viscoelastic foundation. He stated that the Coriolis acceleration term arises because the fluid flows with a velocity relative to the pipe, such that it causes the fluid-structural interaction model to belong to the class of complex eigenvalue problems. It is noted that during free oscillations the Coriolis force term does no work, i.e., it dissipates no energy. This term is also identified as a nonworking velocity-dependent load called gyroscopic by [3, 4]. Confirmation of this is provided by the experimental work reported in [5, 6]. In the 1950s, proofs were claimed of researchers and mathematicians' works that showed that the Coriolis force has negligible effects even at the molecular scale level of interaction. However, it is mentioned that the gyroscopic (Coriolis) forces do no work in the course of free motions, but they nonetheless can exert important influence on the overall dynamical behavior of a pipeline system.

Recent works by Al-Hilli and Ntayeesh (2013) [7] stated that mathematically speaking, the buckling instability of a system arises from the Coriolis term, which represents the forces imposed on the pipe by the flowing fluid that is always 90^{o} out of phase with the pipe displacement, and is always in phase with the

velocity of the pipe. He sees this force as, essentially, a negative damping mechanism, which extracts energy into the bending pipe to encourage initially, vibration, and ultimately buckling. Szmidt and Przybylowicz (2013) [8] studied the influence of electromagnetic damping on the dynamics of a pipe conveying fluid and observed that within such a context, the Coriolis effect is seen to be a destabilizing one. Anklin et al (2006) [9] have also presented overviews about mass flow-meters using the principle of Coriolis force effects.

This paper presents exact closed-form solutions for the complex and natural frequencies, and demonstrates the dependence of the complex frequencies - a result of the Coriolis force - on the natural frequency of the system, and the effects of the force as well as the impact of damping force component on the system are illustrated. For clarity, this paper is organized as follows: Section 1 introduces the problem under investigation with appropriate notations within a general context. Followed by Section 2, in which the analysis of the pipeline system conveying an incompressible fluid is presented and briefly reviewed for the derivation of the governing partial differential equation. In Section 3, the complex and natural frequencies, dynamic responses and logarithmic decrement analysis are derived. Section 4 deals with analysis of results and discussion, while concluding with Section 5 and Section 6 enlists the references.

II. Analysis of the Pipeline System Conveying an Incompressible fluid

An analysis of the bending of beams on a viscoelastic foundation, if based on the Winkler model, is derived from the assumption that the foundation's reaction forces are proportional at every point to the deflection of the beam at that point. The differential equation of the elastic line is based on the assumption that a straight beam is supported along its entire length by a viscoelastic medium and subjected to vertical forces acting in the principal plane of the symmetrical cross section (see Figure 1).

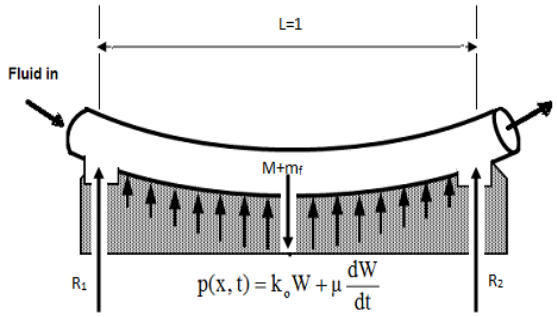

Figure 1: Representation of modified Winkler foundation model

The partial differential equation governing the dynamics of a fluid-conveying pipeline supported on a viscoelastic foundation [2] is given as

$$EI\frac{\partial^4 w}{\partial x^4}+k_0 w+m_f U^2\frac{\partial^2 w}{\partial x^2}+\left(M+m_f\right)\frac{\partial^2 w}{\partial t^2}+\mu\frac{\partial w}{\partial t}+2m_f U\frac{\partial^2 w}{\partial t\partial x}=f\left(t\right) \quad (1)$$

On introducing the following dimensionless parameters viz-a-viz;

$$\left(\tau=L^2\sqrt{\frac{M}{EI}};\overline{W}=\frac{w}{L};\bar{x}=\frac{x}{L};\bar{t}=\frac{t}{\tau};\overline{U}=UL\sqrt{\frac{M}{EI}};\right.$$
$$\left.\zeta_f=\frac{m_f}{M};\ \bar{k}_0=\frac{k_0L^4}{EI};\ \bar{\mu}=\frac{\mu L^2}{\sqrt{\rho_s EI}};\ \bar{f}=\frac{L^3 f}{EI}\right)$$

then, Eqn. (1) is transformed to become

$$\frac{\partial^4\overline{W}}{\partial\bar{x}^4}+\bar{k}_0\overline{W}+\zeta_f\overline{U}^2\frac{\partial^2\overline{W}}{\partial x^2}+\left(1+\zeta_f\right)\frac{\partial^2\overline{W}}{\partial\bar{t}^2}+\bar{\mu}\frac{\partial\overline{W}}{\partial\bar{t}}+2\zeta_f\overline{U}\frac{\partial^2\overline{W}}{\partial\bar{t}\partial\bar{x}}=\bar{f}\left(\bar{t}\right) \quad (2)$$

Thus, the components of Eqn. (2) are defined as follows: the first term is the acceleration due to the restoring force, the second and third are the accelerations due to the foundation stiffness and centrifugal force caused by the internal flow within the pipe respectively, then the fourth term stands for acceleration due to the system's inertia force; and following this are accelerations due to the foundation damping as well as the Coriolis forces.

Now, consider the Fourier complex integral transforms i.e.:

$$\left(F\left\{\overline{W}\left(\bar{x},\bar{t}\right)\right\}=\frac{1}{\sqrt{2\pi}}\int_{-\infty}^{\infty}e^{-i\lambda x}\overline{W}\left(\bar{x},\bar{t}\right)d\bar{x}=\overline{W}\left(\lambda,\bar{t}\right);\right.$$
$$\left.F^{-1}\left\{\overline{W}\left(\lambda,\bar{t}\right)\right\}=\frac{1}{\sqrt{2\pi}}\int_{-\infty}^{\infty}e^{i\lambda\bar{x}}\overline{W}\left(\lambda,\bar{t}\right)d\lambda=\overline{W}\left(\bar{x},\bar{t}\right)\right) \quad (3)$$

where, in this case

$$F\left(\bar{x},\bar{t}\right)=\begin{cases}0 & when\ -\infty\le\bar{x}<0\\ \overline{W}\left(\bar{x},\bar{t}\right) & when\ 0\le\bar{x}\le1\\ 0 & when\ 1<\bar{x}\le\infty\end{cases}$$

Applying the Fourier transform on Eqn. (2) reduces it to an ordinary differential equation of the form,

$$\frac{d^2\overline{W}^F}{d\bar{t}^2}+\frac{i\left(2\lambda\zeta_f\overline{U}-i\overline{\mu}\right)}{\left(1+\zeta_f\right)}\frac{d\overline{W}^F}{d\bar{t}}+\frac{\left(\lambda^4-\zeta_f\overline{U}^2\lambda^2+\bar{k}_0\right)}{\left(1+\zeta_f\right)}\overline{W}^F = \frac{\bar{f}\left(\bar{t}\right)+\begin{pmatrix}-\overline{W}_{\bar{x}\bar{x}\bar{x}}\left(\bar{x},0\right)e^{-i\lambda\bar{x}}\Big|_0^1\\+\left(\lambda^2-\zeta_f U^2\right)\overline{W}_{\bar{x}}\left(\bar{x},0\right)e^{-i\lambda\bar{x}}\Big|_0^1\end{pmatrix}}{\left(1+\zeta_f\right)} \quad (4)$$

When subjected to simple supports at both ends, the following boundary conditions hold,

$$\begin{pmatrix}\overline{W}\left(0,t\right)=\overline{W}_{xx}\left(0,t\right)=0\\\overline{W}\left(1,t\right)=\overline{W}_{xx}\left(1,t\right)=0\end{pmatrix}$$

in conjunction with the conditions of boundary velocities as,

$$\frac{d\overline{W}\left(0,t\right)}{d\bar{t}}=\frac{d\overline{W}\left(1,t\right)}{d\bar{t}}=0$$

This is a non-homogeneous form of a second order ordinary differential equation in the time domain.

III. Complex and Natural frequencies

On introducing the Laplace transforms, viz.,

$$\begin{pmatrix}\Im\left\{\overline{W}\left(\lambda,t\right)\right\}=\int_0^\infty\overline{W}\left(\bar{z},t\right)e^{-st}\,dt=\overline{W}\left(\lambda,s\right);\\\Im^{-1}\left\{\overline{W}\left(\lambda,s\right)\right\}=\frac{1}{2\pi i}\int_{\gamma-i\infty}^{\gamma+i\infty}\overline{W}\left(\lambda,s\right)e^{st}\,ds=\overline{W}\left(\bar{z},t\right)\end{pmatrix} \quad (5)$$

With Eqns. (4) and (5), and setting the initial conditions and other right hand side terms to zero, the following system is deduced,

$$\left(s^2+i\left(\frac{\left(2\lambda\zeta_f\overline{U}-i\overline{\mu}\right)}{\left(1+\zeta_f\right)}\right)s+\frac{\left(\lambda^4-\zeta_f\overline{U}^2\lambda^2+\bar{k}_0\right)}{\left(1+\zeta_f\right)}\right)=0$$

Solving to give complex frequency pairs of the forms;

$$\Omega_1=-\left(\frac{2\lambda\zeta_f\overline{U}-i\overline{\mu}}{2\left(1+\zeta_f\right)}\right)-\sqrt{\left(\frac{2\lambda\zeta_f\overline{U}-i\overline{\mu}}{2\left(1+\zeta_f\right)}\right)^2+\frac{\left(\lambda^4-\zeta_f\overline{U}^2\lambda^2+\bar{k}_0\right)}{\left(1+\zeta_f\right)}} \quad (6)$$

and

$$\Omega_2=-\left(\frac{2\lambda\zeta_f\overline{U}-i\overline{\mu}}{2\left(1+\zeta_f\right)}\right)+\sqrt{\left(\frac{2\lambda\zeta_f\overline{U}-i\overline{\mu}}{2\left(1+\zeta_f\right)}\right)^2+\frac{\left(\lambda^4-\zeta_f\overline{U}^2\lambda^2+\bar{k}_0\right)}{\left(1+\zeta_f\right)}} \quad (7)$$

Further manipulations on these frequency equations give the ,

$$\Omega_1=-\Omega_n\left(\left(\xi-i\frac{\overline{\mu}_c}{2}\right)+\sqrt{1+\left(\xi-\frac{i\overline{\mu}_c}{2}\right)^2}\right) \quad (8)$$

$$\Omega_2=-\Omega_n\left(\left(\xi-i\frac{\overline{\mu}_c}{2}\right)-\sqrt{1+\left(\xi-\frac{i\overline{\mu}_c}{2}\right)^2}\right) \quad (9)$$

where

$$\xi=\frac{\Omega_{cd}}{\Omega_n};\ \overline{\mu}_c=\frac{\overline{\mu}}{\Omega_n};\ \Omega_{cd}=\left(\frac{2\lambda\zeta_f\overline{U}-i\overline{\mu}}{2\left(1+\zeta_f\right)}\right)$$

But, it can be observed that the natural frequency of the system is derivable from Eqns. (8) and (9) as follows,

$${\Omega_n}^2=\Omega_1\times\Omega_2=\frac{\left(\lambda^4-\zeta_f\overline{U}^2\lambda^2+\bar{k}_0\right)}{\left(1+\zeta_f\right)} \quad (10)$$

A. *Dynamic Response Analysis*

Now consider figure 1above. It is shown that with uniformly distributed loads of $\overline{w}g$ Newton per unit length, deflection is symmetric about the middle of the beam (or the pipe) and the governing differential equation for the static state of the pipeline system when time $\bar{t}=0$ and the flow $\overline{U}=0$, is given as

$$\frac{\partial^4\overline{W}}{\partial\bar{x}^4}+\bar{k}_0\overline{W}=\overline{w} \quad (11)$$

On solving Eqn. (11) - Kreyszig (2006), Jeffrey (2002) [10-11], the displacement at $\bar{t}=0$ is given by

$$\overline{W}\left(\bar{x},0\right)=\overline{w}\begin{pmatrix}-\frac{1}{k^2}\left(\frac{\alpha_{14}\beta_{11}-\alpha_{12}\beta_{12}}{\alpha_{11}\alpha_{14}+\alpha_{12}\alpha_{13}}\right)\begin{Bmatrix}(i+1)\sin(i+1)k\bar{x}\\+(i-1)\sin(i-1)k\bar{x}\end{Bmatrix}\\-\frac{1}{2k^3}\left(\frac{\alpha_{13}\beta_{11}+\alpha_{11}\beta_{12}}{\alpha_{11}\alpha_{14}+\alpha_{12}\alpha_{13}}\right)\begin{Bmatrix}(i-1)\sin(i+1)k\bar{x}\\+(i+1)\sin(i-1)k\bar{x}\end{Bmatrix}\\+\frac{1}{8k^4}(i-1)\{\cos(i+1)k\bar{x}-1\}\end{pmatrix} \quad (12)$$

where

$$\alpha_{11}=\frac{1}{k^2}(i+1)\sin(i+1)k+(i-1)\sin(i-1)k$$

$$\alpha_{12}=\frac{1}{2k^3}(i-1)\sin(i+1)k+(i+1)\sin(i-1)k$$

$$\alpha_{13}=(i+1)^3\sin(i+1)k+(i-1)^3\sin(i-1)k$$

$$\alpha_{14}=k\alpha_{11}$$

$$\beta_{11}=\frac{1}{8k^4}(i-1)\{\cos(i+1)k-1\}$$

$$\beta_{12}=\frac{1}{4k^2}(i+1)\cos(i+1)k$$

Now, taking the Laplace transforms of Eqn. (4) gives

$$\left(s^2+\frac{i\left(2\lambda\zeta_f\bar{U}-i\bar{\mu}\right)}{\left(1+\zeta_f\right)}s+\frac{\left(\lambda^4-\zeta_f\bar{U}^2\lambda^2+\bar{k}_0\right)}{\left(1+\zeta_f\right)}\right)\bar{W}^F = \frac{f_0}{s+i\omega}+(s+2\Omega_{cd})H(\lambda)+\frac{J(\lambda)}{\left(1+\zeta_f\right)s} \tag{13}$$

that is,

$$\bar{W}^F(\lambda,s)=\frac{f_0}{(s+i\omega)(s+i\Omega_1)(s+i\Omega_2)}+\frac{(s+2\Omega_{cd})H(\lambda)}{(s+i\Omega_1)(s+i\Omega_2)}+\frac{J(\lambda)}{\left(1+\zeta_f\right)s(s+i\Omega_1)(s+i\Omega_2)} \tag{14}$$

where

$$J_1(\lambda)=\begin{pmatrix}-\bar{W}_{\bar{x}\bar{x}\bar{x}}(\bar{x},0)e^{-i\lambda\bar{x}}\Big|_0^1\\+\left(\lambda^2-\zeta_f U^2\right)\bar{W}_{\bar{x}}(\bar{x},0)e^{-i\lambda\bar{x}}\Big|_0^1\end{pmatrix} \tag{15}$$

$$H(\lambda)=\int_0^1\bar{W}(\bar{x},0)e^{-i\lambda\bar{x}}d\bar{x}=\bar{W}^F(\lambda,0) \tag{16}$$

but

$$\bar{W}_{\bar{x}}(\bar{x},0)=\bar{w}\begin{pmatrix}-\frac{1}{k}\left(\frac{\alpha_{14}\beta_{11}-\alpha_{12}\beta_{12}}{\alpha_{11}\alpha_{14}+\alpha_{12}\alpha_{13}}\right)\\\times\left\{\begin{matrix}(i+1)^2\cos(i+1)k\bar{x}\\+(i-1)^2\cos(i-1)k\bar{x}\end{matrix}\right\}\\+\frac{1}{k^2}\left(\frac{\alpha_{13}\beta_{11}+\alpha_{11}\beta_{12}}{\alpha_{11}\alpha_{14}+\alpha_{12}\alpha_{13}}\right)\\\times\{\cos(i+1)k\bar{x}+\cos(i-1)k\bar{x}\}\\+\frac{1}{4k^4}\sin(i+1)k\bar{x}\end{pmatrix} \tag{17a}$$

$$\bar{W}_{\bar{x}\bar{x}\bar{x}}(\bar{x},0)=\bar{w}\begin{pmatrix}k\left(\frac{\alpha_{14}\beta_{11}-\alpha_{12}\beta_{12}}{\alpha_{11}\alpha_{14}+\alpha_{12}\alpha_{13}}\right)\\\times\left\{\begin{matrix}(i+1)^4\cos(i+1)k\bar{x}\\+(i-1)^4\cos(i-1)k\bar{x}\end{matrix}\right\}\\-\left(\frac{\alpha_{13}\beta_{11}+\alpha_{11}\beta_{12}}{\alpha_{11}\alpha_{14}+\alpha_{12}\alpha_{13}}\right)\\\times\left\{\begin{matrix}(i+1)^2\cos(i+1)k\bar{x}\\+(i-1)^2\cos(i-1)k\bar{x}\end{matrix}\right\}\\-\frac{1}{4k}(i+1)^2\sin(i+1)k\bar{x}\end{pmatrix} \tag{17b}$$

where

$$\bar{w}=\frac{m_p gL^2}{E\hat{I}};\ k=\sqrt[4]{\frac{k_0}{4}}$$

Hence,

$$J_1(\lambda)=\bar{w}\begin{pmatrix}\left\{\left(\lambda^2-\bar{U}^2\zeta_f\right)\Gamma_{13}-\Gamma_{11}\right\}e^{-i\lambda}\\+\Gamma_{12}-\Gamma_{14}\end{pmatrix} \tag{18}$$

Now, taking the inverse Laplace transforms therefore, the system response in the Fourier domain is given by

$$\bar{W}_1^F(\lambda,\bar{t})=\frac{\bar{f}_0}{\left(1+\zeta_f\right)}G_1(\bar{t})+\begin{pmatrix}G_2(\bar{t})\\+2\Omega_{cd}G_3(\bar{t})\end{pmatrix}H(\lambda)+\frac{J_1(\lambda)}{\left(1+\zeta_f\right)}G_4(\bar{t}) \tag{19}$$

where

$$G_1(\bar{t}) = \frac{\begin{matrix}(\Omega_1-\Omega_2)e^{-i\omega\bar{t}} - \left(\Omega_1 e^{-i\Omega_2\bar{t}} - \Omega_2 e^{-i\Omega_1\bar{t}}\right) \\ + \omega\left(e^{-i\Omega_2\bar{t}} - e^{-i\Omega_1\bar{t}}\right)\end{matrix}}{(\Omega_2-\Omega_1)(\xi^2-1)}$$

$$\forall \xi = \frac{\omega}{\Omega_n}$$

$$G_2(\bar{t}) = \frac{\left(\Omega_1 e^{-i\Omega_1\bar{t}} - \Omega_2 e^{-i\Omega_2\bar{t}}\right)}{(\Omega_1-\Omega_2)}$$

$$G_3(\bar{t}) = \frac{i\left(e^{-i\Omega_1\bar{t}} - e^{-i\Omega_2\bar{t}}\right)}{(\Omega_1-\Omega_2)}$$

$$G_4(\bar{t}) = \frac{\left(\Omega_1 e^{-i\Omega_2\bar{t}} - \Omega_2 e^{-i\Omega_1\bar{t}}\right) - (\Omega_1-\Omega_2)}{(\Omega_1-\Omega_2)}$$

Substituting $G_i(\bar{t}) \forall i = 1,...4$ into Eqns. (19) gives the dynamic response in the time-Fourier plane as follows;

$$\begin{aligned}\overline{W}_1^F(\lambda,\bar{t}) = {} & \frac{\Omega_2 e^{-i\Omega_2\bar{t}} - \Omega_1 e^{-i\Omega_1\bar{t}}}{\Omega_1-\Omega_2} \frac{-2\Omega_{cd}\left(e^{-i\Omega_1\bar{t}} - e^{-i\Omega_2\bar{t}}\right)}{} H(\lambda) \\ & + \frac{\begin{matrix}(\Omega_1-\Omega_2)e^{-i\omega\bar{t}} \\ -\left(\Omega_1 e^{-i\Omega_2\bar{t}} - \Omega_2 e^{-i\Omega_1\bar{t}}\right) \\ +\omega\left(e^{-i\Omega_2\bar{t}} - e^{-i\Omega_1\bar{t}}\right)\end{matrix}}{(\Omega_2-\Omega_1)(1+\zeta_f)} (1+\xi^2) \frac{\bar{f}_0}{\Omega_n^2} \\ & - \frac{\left(\Omega_1 e^{-i\Omega_2\bar{t}} - \Omega_2 e^{-i\Omega_1\bar{t}}\right) - (\Omega_1-\Omega_2)}{(\Omega_1-\Omega_2)(1+\zeta_f)} \frac{J(\lambda)}{\Omega_n^2}\end{aligned} \quad (20)$$

where

$$\Omega_n^2 = \frac{\lambda^4 - \lambda^2 \overline{U}^2 \zeta_f + \bar{k}_0}{(1+\zeta_f)}; \ \xi << 1$$

On applying the inverse Fourier transform on Eqn. (20), it becomes

$$\overline{W}_1(\bar{x},\bar{t}) = \frac{1}{\sqrt{2\pi}} \int_{-\infty}^{\infty} \overline{W}_1^F(\lambda,\bar{t}) e^{i\lambda\bar{x}} d\lambda \quad (21)$$

That is,

$$\begin{aligned}\overline{W}_1(\bar{x},\bar{t}) = {} & \int_{-\infty}^{\infty} \frac{\Omega_2 e^{-i\Omega_2\bar{t}} - \Omega_1 e^{-i\Omega_1\bar{t}}}{\Omega_1-\Omega_2} \frac{-2\Omega_{cd}\left(e^{-i\Omega_1\bar{t}} - e^{-i\Omega_2\bar{t}}\right)}{} H(\lambda) e^{i\lambda\bar{x}} d\lambda \\ & + \int_{-\infty}^{\infty} \frac{\begin{matrix}(\Omega_1-\Omega_2)e^{-i\omega\bar{t}} \\ -\left(\Omega_1 e^{-i\Omega_2\bar{t}} - \Omega_2 e^{-i\Omega_1\bar{t}}\right) \\ +\omega\left(e^{-i\Omega_2\bar{t}} - e^{-i\Omega_1\bar{t}}\right)\end{matrix}}{(\Omega_2-\Omega_1)(1+\zeta_f)} (1+\xi^2) \frac{\bar{f}_0}{\Omega_n^2} e^{i\lambda\bar{x}} d\lambda \\ & - \int_{-\infty}^{\infty} \frac{\left(\Omega_1 e^{-i\Omega_2\bar{t}} - \Omega_2 e^{-i\Omega_1\bar{t}}\right) - (\Omega_1-\Omega_2)}{(\Omega_1-\Omega_2)(1+\zeta_f)} \frac{J(\lambda)}{\Omega_n^2} e^{i\lambda\bar{x}} d\lambda\end{aligned} \quad (22)$$

which further gives

$$\begin{aligned}\overline{W}_1(\bar{x},\bar{t}) = {} & \frac{\begin{matrix}\Omega_1 e^{-i\Omega_2\bar{t}} - \Omega_2 e^{-i\Omega_1\bar{t}} \\ -2\Omega_{cd}\left(e^{-i\Omega_1\bar{t}} - e^{-i\Omega_2\bar{t}}\right)\end{matrix}}{\Omega_1-\Omega_2} \\ & \overline{w}\begin{pmatrix} -\frac{1}{k^2}\left(\frac{\alpha_{14}\beta_{11}-\alpha_{12}\beta_{12}}{\alpha_{11}\alpha_{14}+\alpha_{12}\alpha_{13}}\right)\begin{Bmatrix}(i+1)\sin(i+1)k\bar{x} \\ +(i-1)\sin(i-1)k\bar{x}\end{Bmatrix} \\ -\frac{1}{2k^3}\left(\frac{\alpha_{13}\beta_{11}+\alpha_{11}\beta_{12}}{\alpha_{11}\alpha_{14}+\alpha_{12}\alpha_{13}}\right)\begin{Bmatrix}(i-1)\sin(i+1)k\bar{x} \\ +(i+1)\sin(i-1)k\bar{x}\end{Bmatrix} \\ +\frac{1}{8k^4}(i-1)\{\cos(i+1)k\bar{x}-1\}\end{pmatrix} \\ & + \frac{\begin{matrix}(\Omega_1-\Omega_2)e^{-i\omega\bar{t}} \\ -\left(\Omega_1 e^{-i\Omega_2\bar{t}} - \Omega_2 e^{-i\Omega_1\bar{t}}\right) \\ +\omega\left(e^{-i\Omega_2\bar{t}} - e^{-i\Omega_1\bar{t}}\right)\end{matrix}}{\sqrt{\eta}(\Omega_2-\Omega_1)(1+\zeta_f)} (1+\xi^2) \bar{f}_0 \sin\sqrt{\eta}\bar{x} \\ & - i\frac{\left(\Omega_1 e^{-i\Omega_2\bar{t}} - \Omega_2 e^{-i\Omega_1\bar{t}}\right) - (\Omega_1-\Omega_2)}{\sqrt{\eta}(\Omega_1-\Omega_2)(1+\zeta_f)} \\ & \overline{w}\begin{pmatrix}\left\{\mp\left(\frac{\overline{U}^4\zeta_F^2}{4} - \bar{k}_0\right)\Gamma_3 - \Gamma_1\right\}\sin\sqrt{\eta}(1-\bar{x}) \\ +(\Gamma_2-\Gamma_4)\sin\sqrt{\eta}\bar{x}\end{pmatrix}\end{aligned} \quad (23)$$

Then, on enforcing the initial conditions $\overline{W}(0,\bar{t}) = \overline{W}(1,\bar{t}) = 0$ and $\overline{W}_{\bar{x}\bar{x}}(0,\bar{t}) = \overline{W}_{\bar{x}\bar{x}}(1,\bar{t}) = 0$,the response equation (23) finally becomes

$$\overline{W}_1(\bar{x},\bar{t}) = \frac{\begin{pmatrix}\Omega_1 e^{-i\Omega_2\bar{t}} - \Omega_2 e^{-i\Omega_1\bar{t}} \\ -2\Omega_{cd}\left(e^{-i\Omega_1\bar{t}} - e^{-i\Omega_2\bar{t}}\right)\end{pmatrix}}{\Omega_1 - \Omega_2}$$

$$\overline{w}\begin{pmatrix} -\frac{1}{k^2}\left(\frac{\alpha_{14}\beta_{11}-\alpha_{12}\beta_{12}}{\alpha_{11}\alpha_{14}+\alpha_{12}\alpha_{13}}\right)\begin{Bmatrix}(i+1)\sin(i+1)k\bar{x} \\ +(i-1)\sin(i-1)k\bar{x}\end{Bmatrix} \\ -\frac{1}{2k^3}\left(\frac{\alpha_{13}\beta_{11}+\alpha_{11}\beta_{12}}{\alpha_{11}\alpha_{14}+\alpha_{12}\alpha_{13}}\right)\begin{Bmatrix}(i-1)\sin(i+1)k\bar{x} \\ +(i+1)\sin(i-1)k\bar{x}\end{Bmatrix} \\ +\frac{1}{8k^4}(i-1)\{\cos(i+1)k\bar{x}-1\}\end{pmatrix}$$

$$+i\frac{\begin{Bmatrix}(\Omega_1-\Omega_2)e^{-i\omega\bar{t}} \\ -\left(\Omega_1 e^{-i\Omega_2\bar{t}} - \Omega_2 e^{-i\Omega_1\bar{t}}\right) \\ +\omega\left(e^{-i\Omega_2\bar{t}} - e^{-i\Omega_1\bar{t}}\right)\end{Bmatrix}(1+\xi^2)}{n\pi(\Omega_2-\Omega_1)(1+\zeta_f)}\bar{f}_0\sin n\pi\bar{x}$$

$$-i\frac{\left(\Omega_1 e^{-i\Omega_2\bar{t}} - \Omega_2 e^{-i\Omega_1\bar{t}}\right)-(\Omega_1-\Omega_2)}{n\pi(\Omega_1-\Omega_2)(1+\zeta_f)}$$

$$\times\overline{w}\begin{pmatrix}\begin{Bmatrix}\mp\left(\frac{\overline{U}^4\zeta_F^2}{4}-\bar{k}_0\right)\Gamma_3-\Gamma_1\end{Bmatrix}\sin n\pi(1-\bar{x}) \\ +(\Gamma_2-\Gamma_4)\sin n\pi\bar{x}\end{pmatrix} \quad (24)$$

where

$$\xi << 1$$

$$\begin{pmatrix}\Gamma_1 = \begin{Bmatrix}k\left(\frac{\alpha_{14}\beta_{11}-\alpha_{12}\beta_{12}}{\alpha_{11}\alpha_{14}+\alpha_{12}\alpha_{13}}\right)\gamma_4 \\ -\left(\frac{\alpha_{13}\beta_{11}+\alpha_{11}\beta_{12}}{\alpha_{11}\alpha_{14}+\alpha_{12}\alpha_{13}}\right)\gamma_5-\frac{1}{4k}\gamma_6\end{Bmatrix} \\ \Gamma_2 = \begin{Bmatrix}k\left(\frac{\alpha_{14}\beta_{11}-\alpha_{12}\beta_{12}}{\alpha_{11}\alpha_{14}+\alpha_{12}\alpha_{13}}\right)\{(i-1)^4+(i+1)^4\} \\ -\left(\frac{\alpha_{13}\beta_{11}+\alpha_{11}\beta_{12}}{\alpha_{11}\alpha_{14}+\alpha_{12}\alpha_{13}}\right)\{(i-1)^2+(i+1)^2\}\end{Bmatrix} \\ \Gamma_3 = \begin{pmatrix}-\frac{1}{k}\left(\frac{\alpha_{14}\beta_{11}-\alpha_{12}\beta_{12}}{\alpha_{11}\alpha_{14}+\alpha_{12}\alpha_{13}}\right)\gamma_1 \\ +\frac{1}{k^2}\left(\frac{\alpha_{13}\beta_{11}+\alpha_{11}\beta_{12}}{\alpha_{11}\alpha_{14}+\alpha_{12}\alpha_{13}}\right)\gamma_2+\frac{1}{4k^3}\gamma_3\end{pmatrix} \\ \Gamma_4 = -\frac{1}{k}\left(\frac{\alpha_{14}\beta_{11}-\alpha_{12}\beta_{12}}{\alpha_{11}\alpha_{14}+\alpha_{12}\alpha_{13}}\right)\{(i-1)^2+(i+1)^2\}\end{pmatrix}$$

and

$$\gamma_1 = (i+1)^2\cos(i+1)k + (i-1)^2\cos(i-1)k$$
$$\gamma_2 = \cos(i+1)k + \cos(i-1)k$$
$$\gamma_3 = \sin(i+1)k$$
$$\gamma_4 = (i+1)^4\cos(i+1)k + (i-1)^4\cos(i-1)k$$
$$\gamma_5 = \gamma_1$$
$$\gamma_6 = (i+1)^2\gamma_3$$

With the characteristic equation of the system when $\bar{x} = 0$ *or* 1 given as

$$\sin\sqrt{\eta} = 0 \quad (25)$$

and, from Eqn. (25), it is shown that

$$\sqrt{\eta} = n\pi \Rightarrow \eta = \left(\frac{\overline{U}^2\zeta_f}{2} \pm \sqrt{\frac{\overline{U}^4\zeta_f^2 - 4k_0}{4}}\right)$$

thus,

$$\overline{U}_{cr} = \sqrt{\frac{n^2\pi^2}{\zeta_f} + \frac{k_0}{n^2\pi^2\zeta_f}} \quad (26)$$

Then, as the stiffness k_0 tends to zero, the critical flow velocity turns to the result for a system supported above a foundation, viz.

$$\overline{U}_{cr} = \frac{n\pi}{\sqrt{\zeta_f}} \quad \forall n = 1,2,... \quad (27)$$

B. Logarithmic Decrement Analysis

All real systems dissipate energy when they vibrate. The energy dissipated is often very small, so that an undamped analysis is sometimes realistic; but when the damping is significant its effects must be included in the analysis, particularly when the amplitude of vibration is required. Energy is dissipated by frictional effects, as in the case of the pipeline system resting on the viscoelastic foundation. Common types of damping are viscous, dry friction and hysteretic, however, a convenient way of determining the damping in a system is to measure the rate of decay of oscillation. Thus, logarithmic decrement, the natural logarithm of the ratio of any two successive amplitudes in the same direction can be applied [13]. The logarithmic damping coefficient is used as a measure of the damping capacity of a structure. Here, the effect of span on a fluid-conveying pipeline damping capacity is particularly observed and investigated via the characteristics of the decrement with the flow velocity and time.

Recall from Eqns. (4), (8) and (11) that the homogeneous form of the governing equation can be written as

$$\frac{d^2\overline{W}^F}{d\bar{t}^2}+2\Omega_{cd}\frac{d\overline{W}^F}{d\bar{t}}+\Omega_n^2\overline{W}^F=0 \qquad (28)$$

Using $\overline{W}^F=e^{\Omega\bar{t}}\cdot\overline{Z}$ as $\Omega\to-\Omega_{cd}$ transforms Eqn. (28) to the following

$$\frac{d^2\overline{Z}}{d\bar{t}^2}+\mu^2\overline{Z}=0 \qquad (29)$$

where

$$\mu^2=\Omega^2-\Omega_{cd}^2$$

and, the solution to Eqn. (29) is $\overline{Z}=A\cos(\mu\bar{t}+\varepsilon)$, hence Eqn. (28) is solved to become

$$\overline{W}^F=e^{-\Omega_{cd}\bar{t}}\cdot A\cos(\mu\bar{t}+\varepsilon) \qquad (29)$$

This may represent typical simple harmonic motion, with its amplitude diminishing exponentially to zero as the time $\bar{t}$ increases. Now, if we start measuring the motion when the phase angle $\varepsilon=0$, i.e. $\overline{W}^F=A$, thus

$$\overline{W}^F=e^{-\Omega_{cd}\bar{t}}\cdot A\cos\mu\bar{t} \qquad (30)$$

When $\overline{W}^F=0$, then $\cos\mu\bar{t}=0$ i.e. $\mu\bar{t}=(2n-1)\pi/2$, and when $d\overline{W}^F/d\bar{t}=0$, $\tan\mu\bar{t}=-\Omega_{cd}/\mu$ thus comparing two successive amplitudes gives the Amplitude Reduction Ratio (ARR) of the system as follows,

$$ARR=\frac{\overline{W}_{\tau+1}^F}{\overline{W}_{\tau}^F}=-e^{-\Omega_{cd}(\bar{t}_{\tau+1}-\bar{t}_{\tau})}=-e^{-\frac{\Omega_{cd}\pi}{\mu}} \qquad (31)$$

Now, from the given ARR, i.e. Eqn. (31), the logarithmic decrement of the motion can be deduced as

$$\ln\frac{\overline{W}_{\tau+1}^F}{\overline{W}_{\tau}^F}=\frac{2\Omega_{cd}\pi}{\sqrt{\Omega^2-\Omega_{cd}^2}} \qquad (32)$$

Hence, from Eqn. (32) and for the even modes, we write the logarithmic damping for the mid-position of the system as

$$\delta=\ln\left\{\frac{\overline{W}\left(\frac{1}{2},\tau\right)}{\overline{W}\left(\frac{1}{2},\tau+1\right)}\right\} \qquad (33)$$

III. Results Analyses

In this paper, the mechanics of a fluid-conveying pipe line system resting on a viscoelastic foundation is investigated. The analysis of the initial-boundary value problem modeled to represent this system was done via powerful operational methods, that is, by using the integral transforms to solve the problem therefore making it possible to observe many mathematical and physical applications of the system. To start with, the relationship between the internal flow velocity and the real and imaginary parts of the system's complex frequencies are demonstrated in figures (2-4), for various values of (i) the foundation stiffness constant, (ii) the fluid-pipe mass ratio and (iii) the mode's number. Figures 2 (a) and (b) show families of curves in which the critical flow velocity is depicted as increasing with increasing foundation stiffness constant, whereas in figures 3(a) and (b), the critical flow decreases with increasing fluid-pipe mass ratio, but as for increasing the number of modes, the critical flow increases. (Figures 4 (a) and (b)).

The graphs illustrated by figures(5-7) are for the real, the imaginary parts and the absolute values of the system's natural frequencies as functions of the dimensionless flow velocities. The two domains of the flows, (see figures 5 (a), (b), 6(a), (9b) and 7(a), (b)), picture the pre-critical and post-critical flow regimes. While the families of curves for the real or the imaginary parts of natural frequency against the flow velocity depict that the critical flows occur as the natural frequencies drop to zero from maximum values or rise from zero to some maximum values respectively, the family of curves for the absolute values of the natural frequency shows that the critical flows are determinable at some low values of the natural frequency other than zero. Also, just as in the cases of the system's complex frequencies, the critical flow velocity increases as the foundation stiffness constant or the number of modes increases, but decreases with increasing fluid-pipe mass ratio.

The system's dynamic responses are next shown as satisfying the boundary conditions and also demonstrating the operational processes of the system as it is excited from its initial configuration when charged dynamically. Figures 8-10 illustrate the dynamic response against the dimensionless pipe length for various values of the foundation stiffness constant, the fluid-pipe mass ratio and the number of modes. The families of curves show the magnitude of the amplitude and the phases of travel for various parameter values, and the number of turning points for different modal values. Depicted in figures 11-17 are the characteristics of the response as a function of time, watching the pipeline segment at its mid-position

– where the maximum deflection is observable. The displayed beat phenomena in these figures are the results of coupled oscillating components within the system. It is clearly noted that transfer of energies occurred between two oscillators in these situations. Thus, energy is being transferred between the components driven by the fast moving natural frequency and the one driven by the slow moving frequency due to the Coriolis and damping forces. Therefore, the latter responses envelope the former, just as shown in the figures.

A. Graphs of complex and natural frequencies

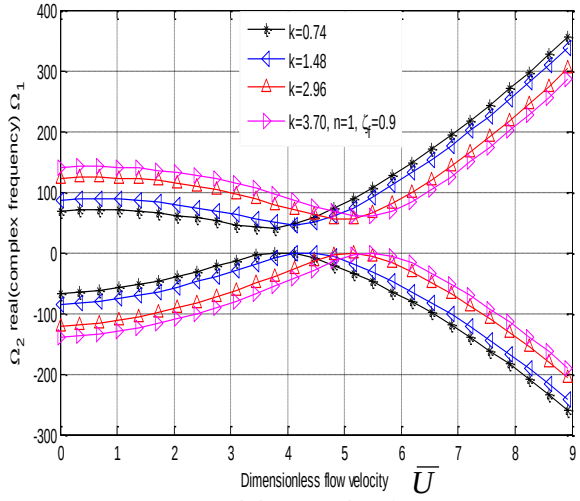

(a) Graph of $real\ part\ of\ \left(-\Omega_{cd} \pm \sqrt{\Omega_{cd}^2 + \Omega_n^2}\right)$

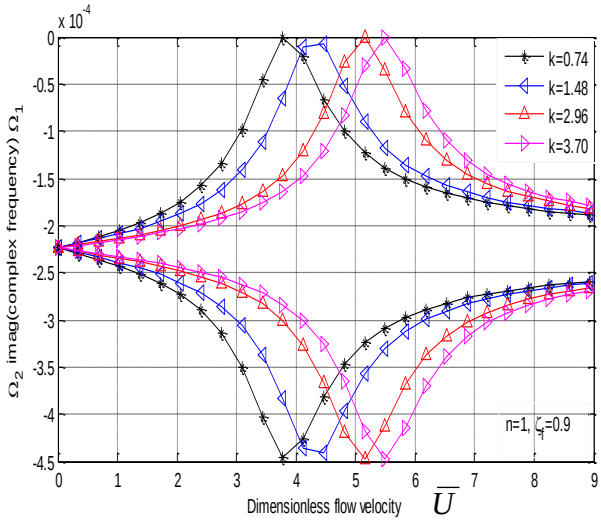

(b) Graph of $imaginary\ part\ of\ \left(-\Omega_{cd} \pm \sqrt{\Omega_{cd}^2 + \Omega_n^2}\right)$

Figure 2: Complex frequency profile

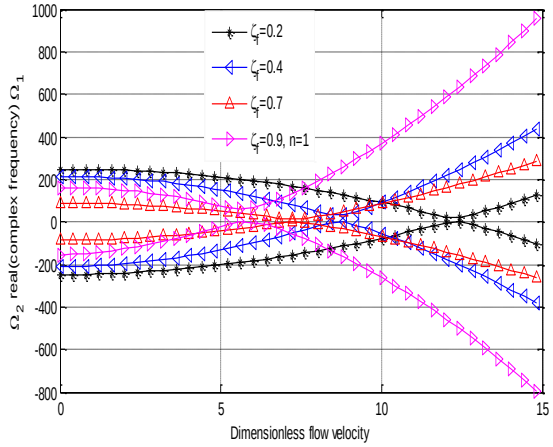

(a) Graph of $real\ part\ of\ \left(-\Omega_{cd} \pm \sqrt{\Omega_{cd}^2 + \Omega_n^2}\right)$

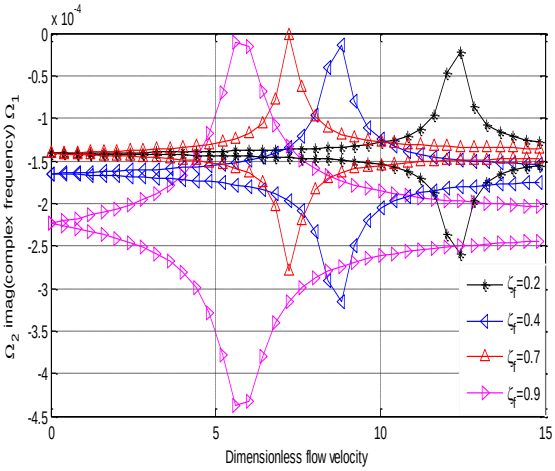

(b) Graph of $imaginary\ part\ of\ \left(-\Omega_{cd} \pm \sqrt{\Omega_{cd}^2 + \Omega_n^2}\right)$

Figure 3: Complex frequency profile

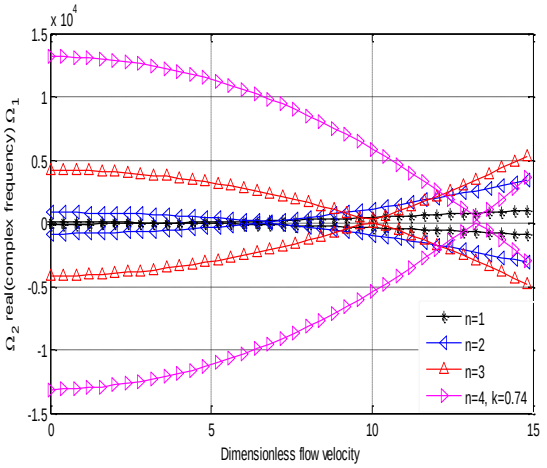

(a) Graph of *real part of* $\left(-\Omega_{cd} \pm \sqrt{\Omega_{cd}^2 + \Omega_n^2}\right)$

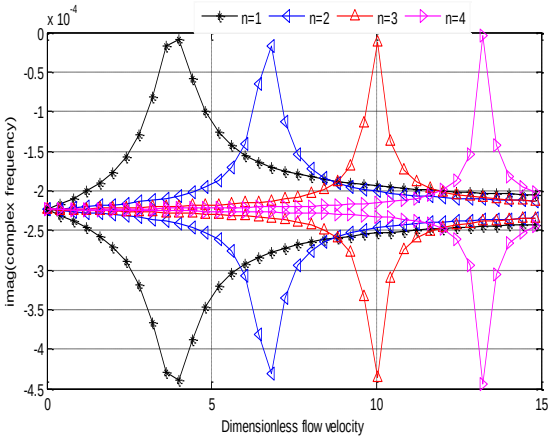

(b) Graph of *imaginary part of* $\left(-\Omega_{cd} \pm \sqrt{\Omega_{cd}^2 + \Omega_n^2}\right)$

Figure 4: Complex frequency profile

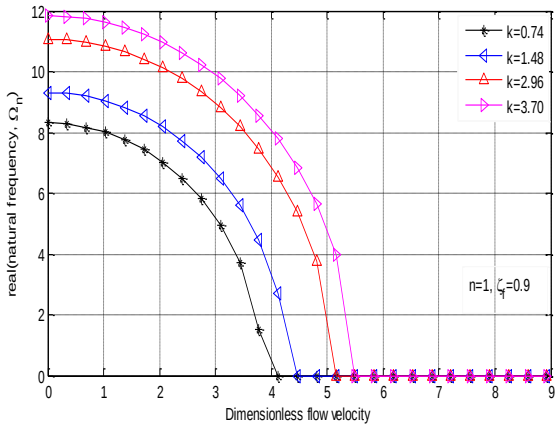

(a) Graph of *real part of* (Ω_n)

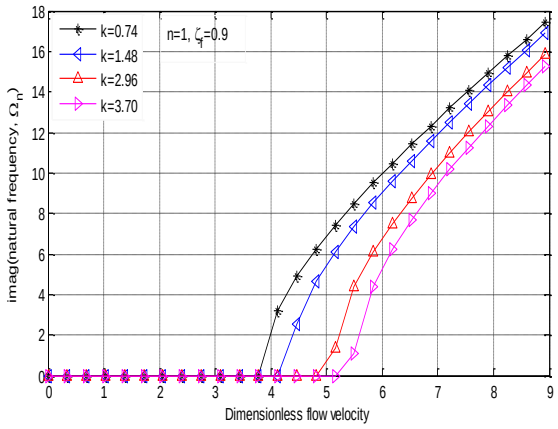

(b) Graph of *imaginary part of* (Ω_n)

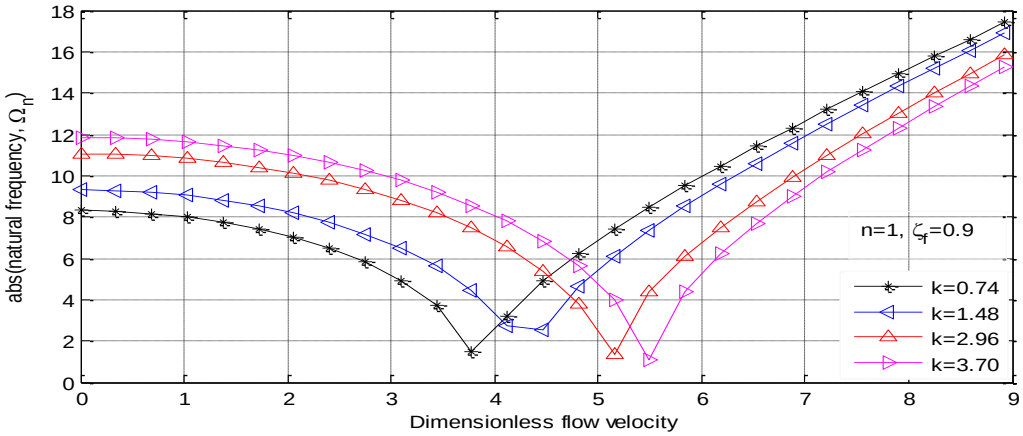

(c) Graph of $\|(\Omega_n)\|$

Figure 5: Natural frequency profile

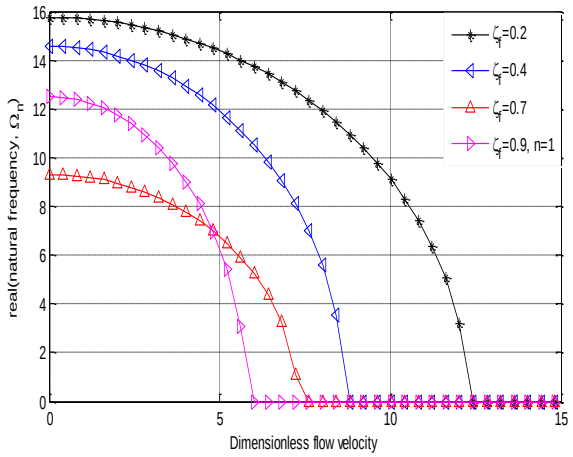

(a) Graph of *real part of* (Ω_n)

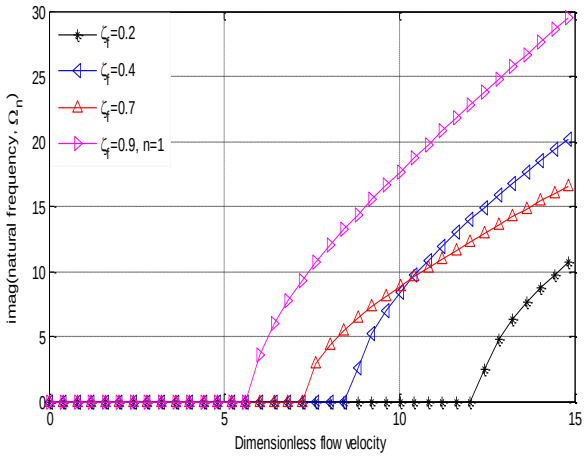

(b) Graph of *imaginary part of* (Ω_n)

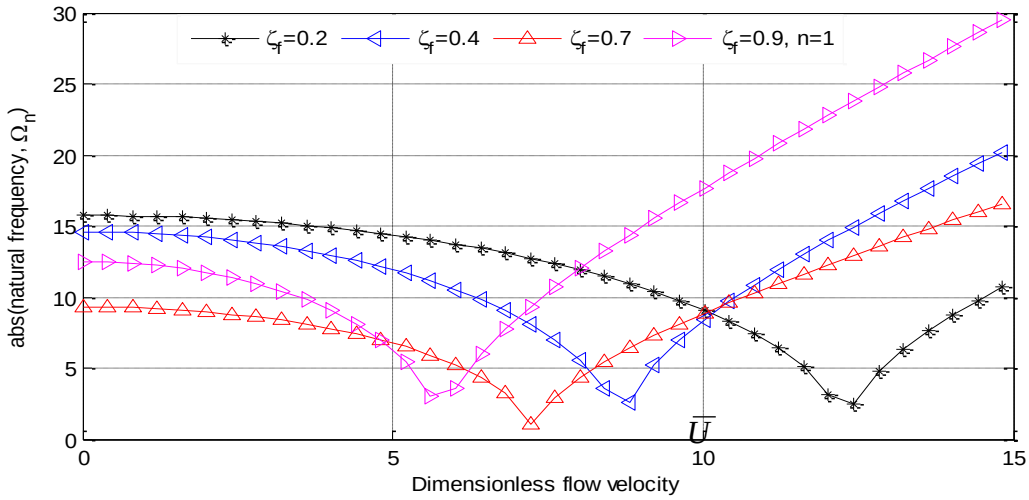

(c) Graph of $\|(\Omega_n)\|$

Figure 6: Complex frequency profile

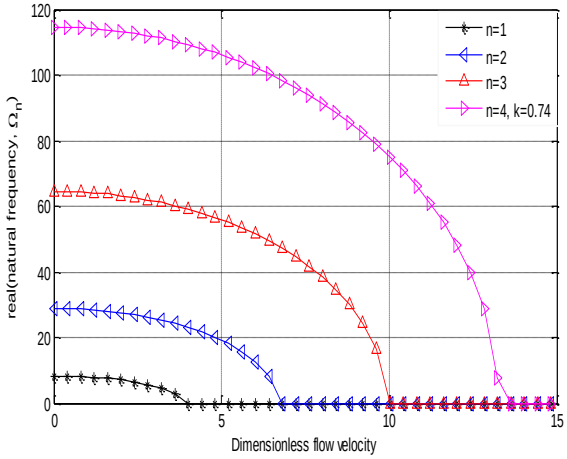

(a) Graph of *real part of* (Ω_n)

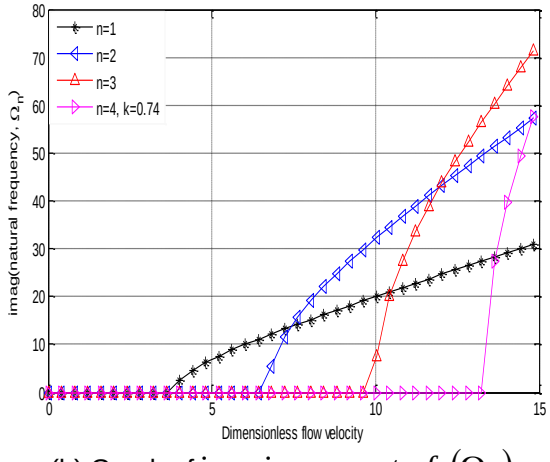

(b) Graph of *imaginary part of* (Ω_n)

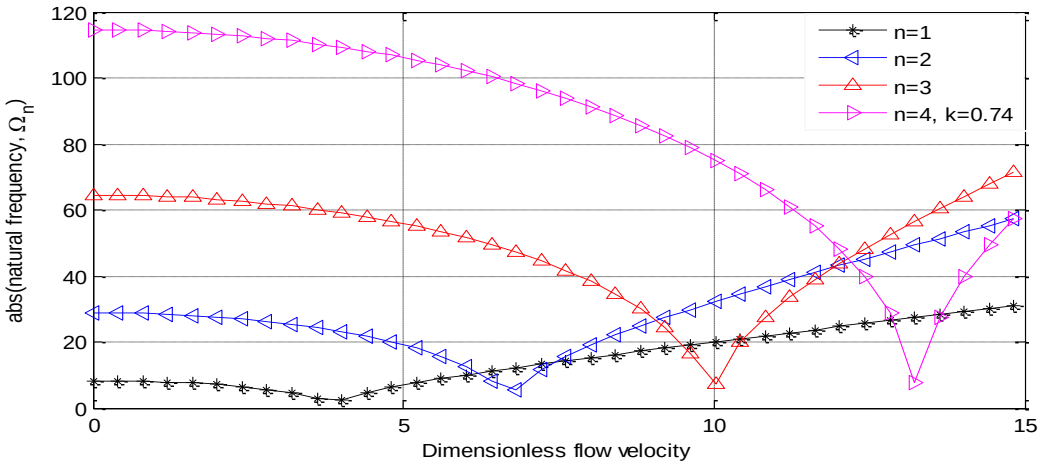

(c) Graph of $\|(\Omega_n)\|$

Figure 7: Natural frequency profile

C. Graphs of system's dynamic responses

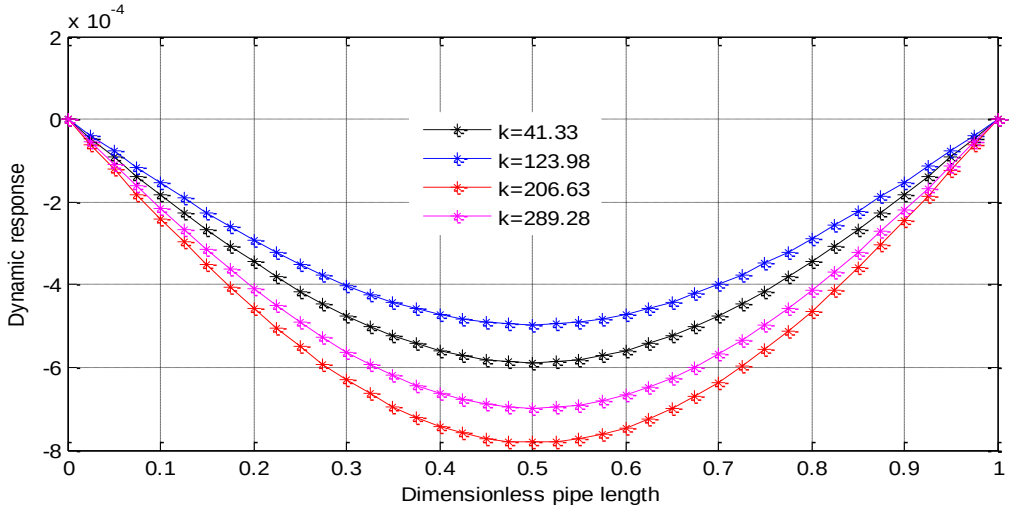

Figure 8: Graph of dynamic response against pipe length

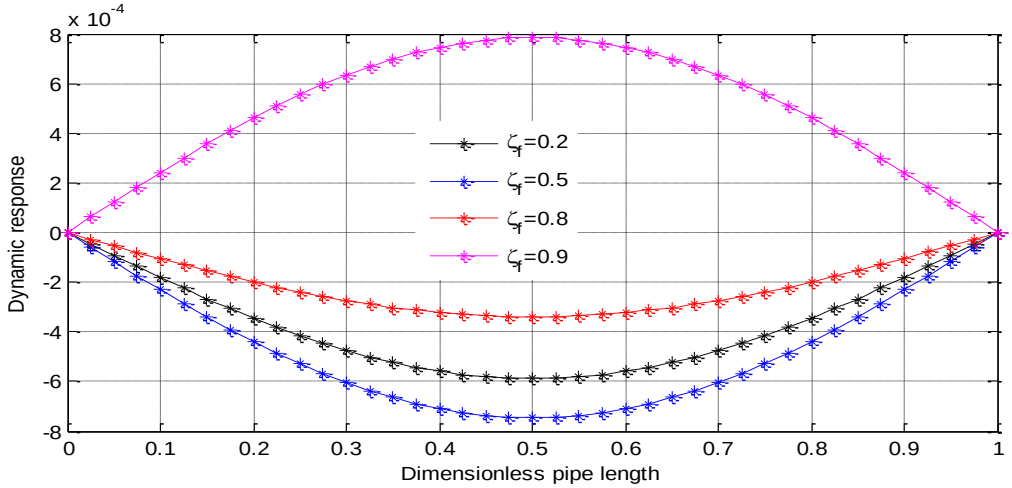

Figure 9: Graph of dynamic response against pipe length

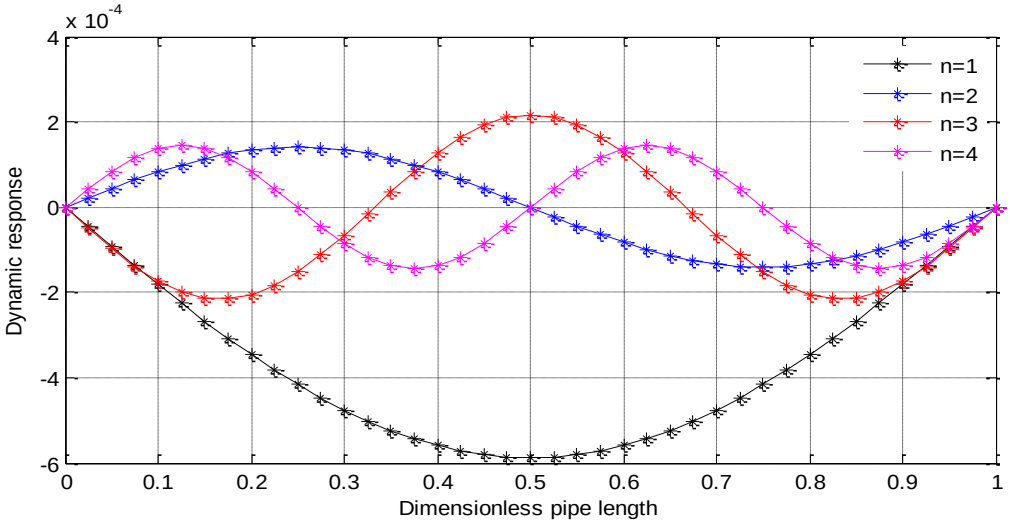

Figure 10: Graph of dynamic response against pipe length

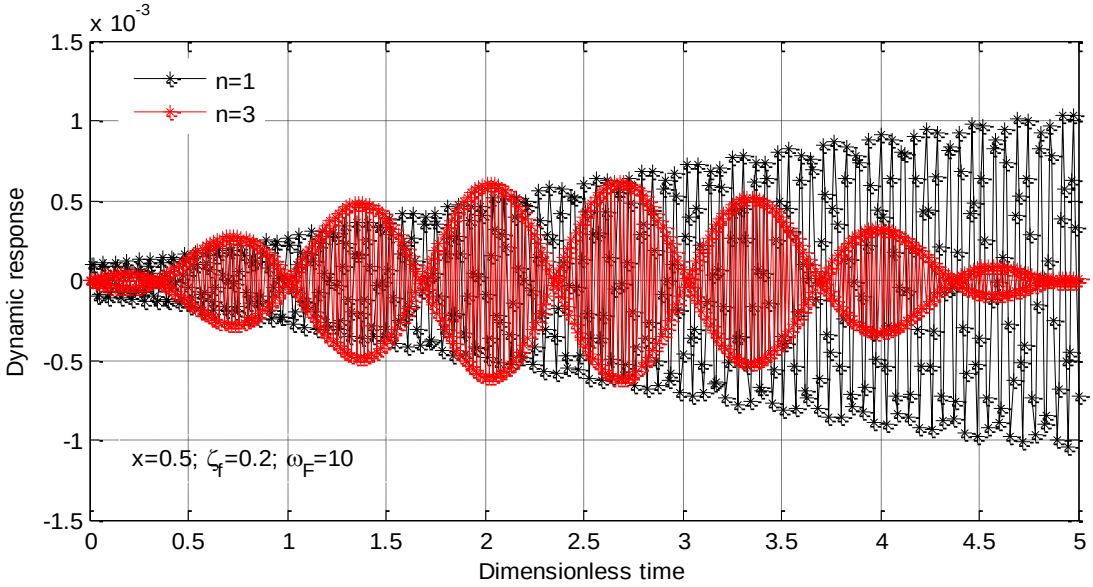

Figure 11: Graph of dynamic response against time

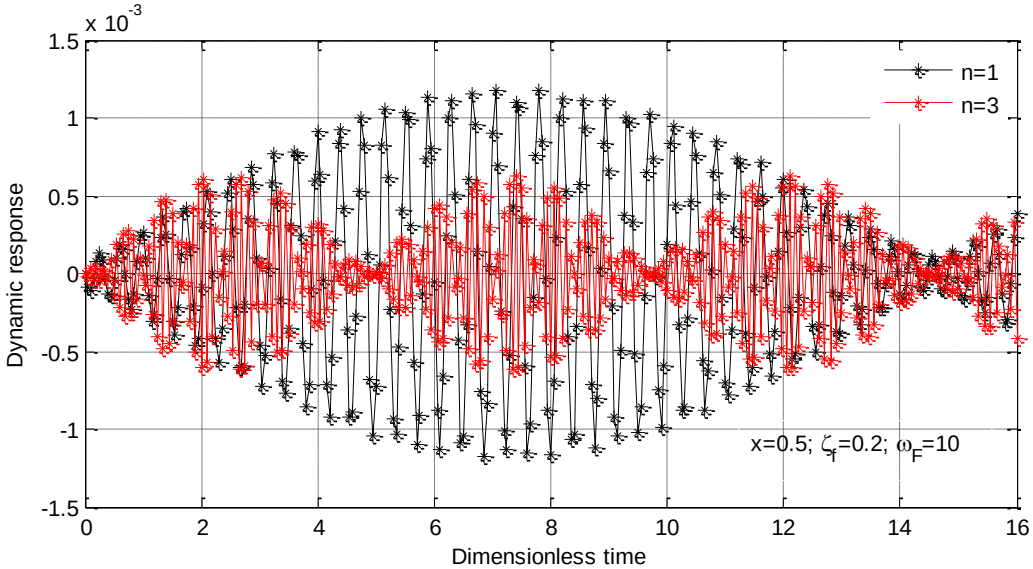

Figure 12: Graph of dynamic response against time

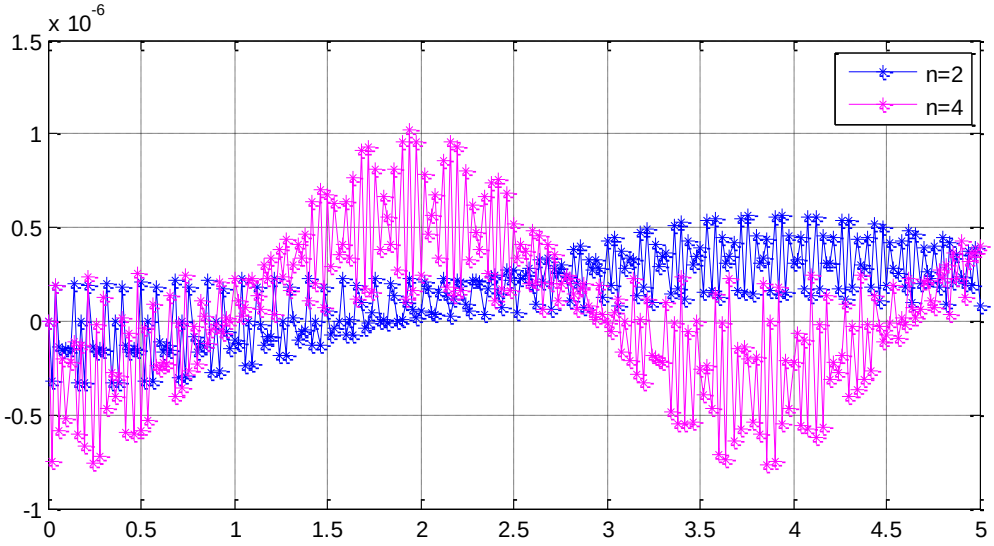

Figure 13: Graph of dynamic response against time

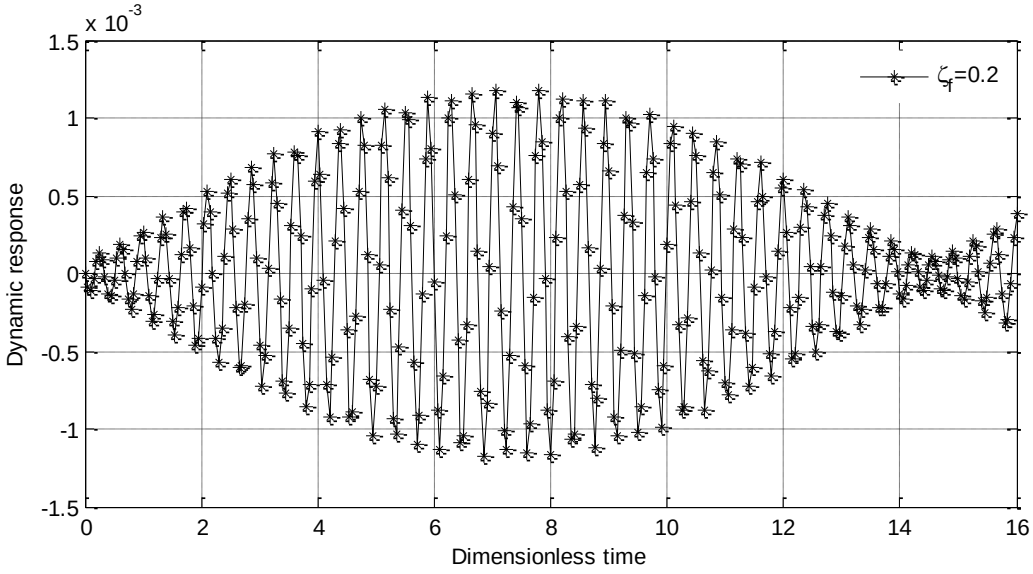

Figure 14: Graph of dynamic response against time

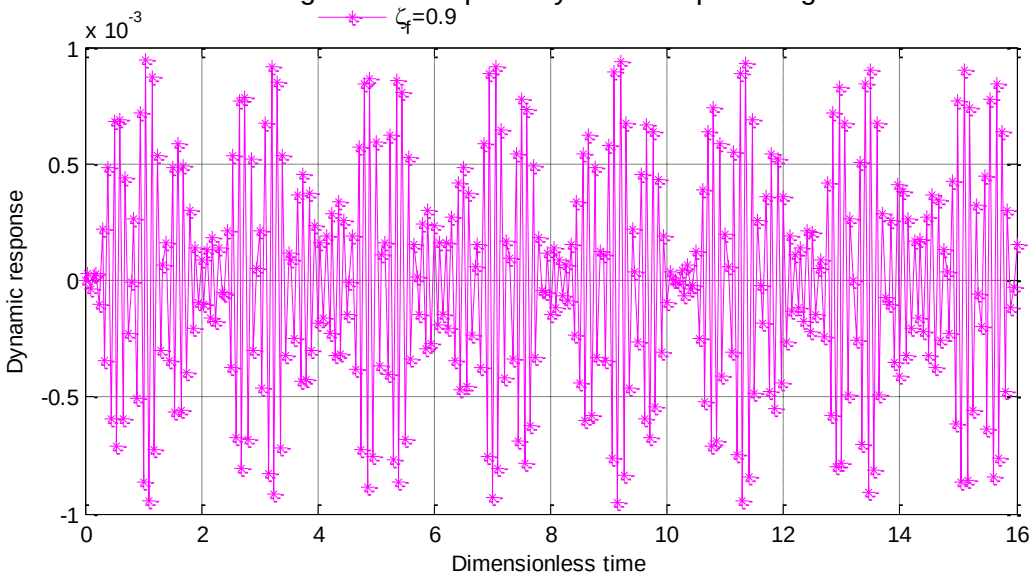

Figure 15: Graph of dynamic response against time

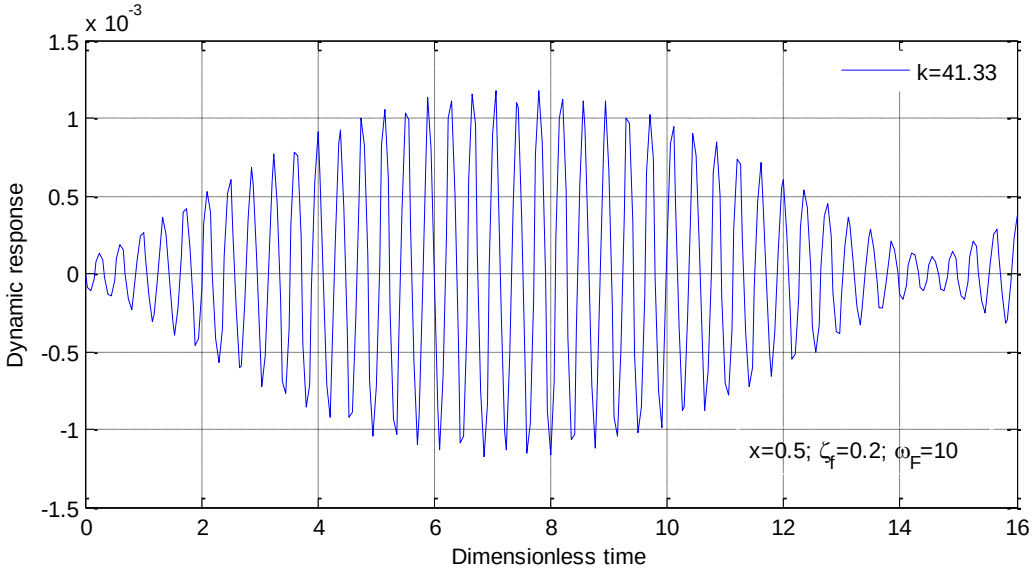

Figure 16: Graph of dynamic response against time

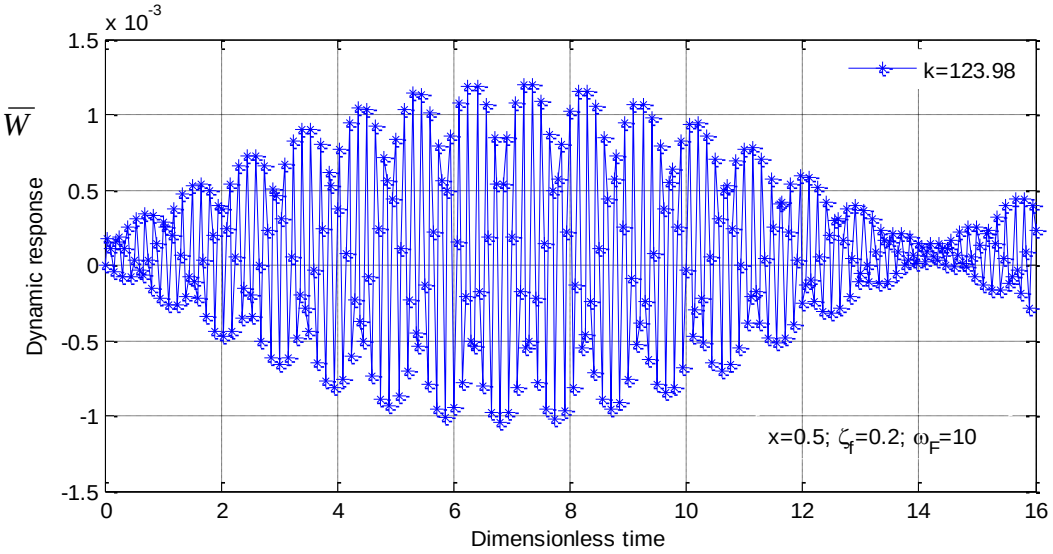

Figure 17: Graph of dynamic response against time

REFERENCES

[1] Paidoussis, M.P. (1998) Fluid-structure interactions: slender structures and axial flows, Vol. 1 Academic Press.

[2] Mostafa N.H. (2014) "Effect of a Viscoelastic foundation on the Dynamic Stability of a Fluid Conveying Pipe". International Journal of Applied Science and Engineering 12, 1:59-74.

[3] Paidoussis, M.P. &Issid, N.T. (1974) Dynamic stability of pipes conveying fluid. Journal of Sound and Vibration 33, 267-294.

[4] Ziegler, H. (1968) Principles of Structural Stability. Waltham, MA: Blaisdell.

[5] Murai, M. and Yamamoto, M. "An Experimental Analysis of the Internal Flow Effects on Marine Risers". Proceedings of MARTEC 2010, P.159-165.

[6] Marakala N, Appukutttan K.K, and Kadoli R. (2014) "Experimental and Theoretical Investigation of Combined Effects of Fluid and Thermal Induced Vibration on Vertical Thin Slender Tube". IOSR- JMCE, ISSN: 2278-1684,pp: 63-68.

[7] Al-Hilli A.H. and Ntayeesh T.J. (2013) "Free Vibration Characteristics of Elastically Supported Pipe Conveying Fluid". NUCEJ vol. 16 No. 1 pp. 9-19.

[8] Szmidt T and Przybylowicz P. (2013) "Critical Flow Velocity with Electromagnetic Actuators". Journal of Theoretical and Applied Mechanics 51, 2, pp. 487-496.

[9] Anklin M., Drahm W. and Rieder A. (2006) Coriolis Mass Flowmeter: Overview of the current state of the art and latest research. Elsevier Flow Measurement and Instrumentation, 17, 317-323.

[10] Kreyzsig E. (2006), Advanced Engineering Mathematics, 9th Edition, John Wiley & Sons, Inc. U.S.A

[11] Jeffrey A. (2002) Advanced Engineering Mathematics, Harcourt Academic Press. U.S.A

[12] Cole E.B. (1960) Theory of Vibrations. The University of Liverpool.

NORMENCLATURE

E Young's modulus
I moment of inertia
ρ_s mass density of pipe per unit length
ρ_f mass density of fluid per unit length
U internal flow velocity
$\overline{w}$ Dead weight of pipe and content
$\overline{W}$ dimensionless dynamic response
$\overline{W}_{\bar{x}}$ pipe's end slope
$\overline{W}_{\bar{x}\bar{x}}$ pipe's end moment
$\overline{W}_{\bar{x}\bar{x}\bar{x}}$ pipe's end shear force
δ logarithmic damping decrement
ARR Amplitude Reduction Ratio
$\bar{t}$ dimensionless time
$\bar{x}$ coordinate of pipe's neutral axis
g gravitational acceleration
L pipe length
λ wave number
ζ_f fluid-pipe mass ratio
ω excitation forcing frequency
Ω_n natural frequency
Ω_1 complex frequency
Ω_2 conjugate complex frequency
Ω_{cd} frequency due to Coriolis and damping forces
$\overline{U}_{cr}$ critical flow velocity

Table: Values of Coding Parameters

Pipe length	100m
External radius	203mm
Internal radius	193mm
Density of pipe material	781kg/m^3
Density of fluid	850 kg/m^3
Elastic constant of pipe material	200x10^{9}Pa
Coefficient of friction	0.04
Excitation force	10KN
Foundation stiffness constant	1KN/m
Excitation force frequency	10rad/s